Bull. Chem. Soc. Ethiop. **2024**, 38(6), 1803-1814.
DOI: https://dx.doi.org/10.4314/bcse.v38i6.23

ISSN 1011-3924
Printed in Ethiopia
Online ISSN 1726-801X

STRUCTURAL, SPECTROSCOPIC, AND MORPHOLOGICAL CHARACTERIZATIONS OF METAL-BASED COMPLEXES DERIVED FROM THE REACTION OF 1-PHENYL-2-THIOUREA WITH Sr^{2+}, Ba^{2+}, Cr^{3+}, AND Fe^{3+} IONS

Mohammed Alsawat[1], Abdel Majid A. Adam[1*], Moamen S. Refat[1], Amnah Mohammed Alsuhaibani[2] and Mohamed Y. El-Sayed[3]

[1]Department of Chemistry, College of Science, Taif University, P.O. Box 11099, Taif 21944, Saudi Arabia
[2]Department of Physical Sport Science, College of Sport Sciences & Physical Activity, Princess Nourah bint Abdulrahman University, P.O. Box 84428, Riyadh 11671, Saudi Arabia
[3]Department of Chemistry, College of Science, Jouf University, Sakaka 2014, Saudi Arabia

(Received July 18, 2024; Revised August 30, 2024; Accepted September 6, 2024)

ABSTRACT. The chemical reaction between 1-phenyl-2-thiourea as a ligand (termed PTU) with the metal ions Sr^{2+}, Ba^{2+}, Cr^{3+}, and Fe^{3+} at a stoichiometry of 2:1 (PTU to metal ion) at 65 °C generated thermally stable metal-based complexes. The synthesized complexes were termed as Complex 1 (Sr^{2+}), Complex 2 (Ba^{2+}), Complex 3 (Cr^{3+}), and Complex 4 (Fe^{3+}). Elemental analyses, thermogravimetry (TG), Fourier-transform infrared (FT-IR) and ultraviolet/visible (UV-Visible) data suggested that the synthesized complexes can be formulated as $[Sr(PTU)_2(H_2O)_4]\cdot Cl_2$ (Complex 1), $[Ba(PTU)_2(H_2O)_4]\cdot Cl_2$ (Complex 2), $[Cr(PTU)_2(H_2O)_2Cl_2]\cdot Cl\cdot 4H_2O$ (Complex 3), $[Fe(PTU)_2(H_2O)_2Cl_2]\cdot Cl\cdot 4H_2O$ (Complex 4). The corresponding gross formulas for these complexes were $C_{14}H_{24}N_4S_2O_4Cl_2Sr$ (534.96 g/mol), $C_{14}H_{24}N_4S_2O_4Cl_2Ba$ (584.23 g/mol), $C_{14}H_{28}N_4S_2O_6Cl_3Cr$ (570.79 g/mol), and $C_{14}H_{28}N_4S_2O_6Cl_3Fe$ (574.63 g/mol), respectively. The X-ray diffraction and scanning electron microscope data demonstrated that the complexes exhibited high purity and possessed a uniform and well-structured morphology.

KEY WORDS: 1-Phenyl-2-thiourea, Metal ion, Thermal decomposition, SEM, Morphology

INTRODUCTION

Transition and non-transition metal ions form a very important class of chemical compounds when reacted with organic molecules. This class of compounds is known as metal-based complexes. It gains considerable interest if the organic molecules possess biological active properties. The reaction of metal ions and drugs led to a critical type of metal-based complexes known as metallodrugs or metal-based drugs. Metal-based complexes and drugs have wide applications in many important fields, such as chemistry, material sciences, physics, biology, catalysis, medicine, and pharmacology [1-12]. Numerous metal-based complexes, such as platinum-based complexes, exhibit potential biological activities (i.e., anticancer, antiviral, antibacterial, antifungal). Platinum complexes are used in cancer therapy in many solid tumors (i.e., ovarian, bladder, testicular) [13-16]. In addition, metal-based complexes are used to treat diabetes, inflammation, neurological disorders, and infection control [17-19]. Several reasons are motivating chemists and pharmacists to investigate, develop, and design novel metal-based complexes and metallodrugs such as: i) to treat new diseases such as coronavirus disease (COVID-19); ii) to overcome adverse side effects of current metallodrugs; iii) to reduce drug resistance; and iv) to enhance the pharmaceutical and biological profiles of several bioactive molecules and drugs. One class of nitrogen and sulfur-containing compounds is thiourea. Thioureas, also known as thiocarbamides, is a class of organic compounds containing three functional groups: thiol (C=S), amino ($-NH_2$), and imino (-NH-), and each of these groups has important biological roles. These three functional

*Corresponding authors. E-mail: majidadam@tu.edu.sa

groups give thiourea a wide range of interesting physico-chemical characteristics. Thiourea has a structural resemblance to urea, except that a sulfur atom replaces urea's oxygen atom, and this change makes the chemical properties of thiourea quite different from urea. Thiourea has a wide range of applications in agriculture, medicine, analytical chemistry, metallurgy, and industry [20-22].

In this study, we aim to provide new insights into the complexation behavior of one member from the thiourea family: 1-phenyl-2-thiourea (termed PTU). First, the chemical reaction of PTU with the metal ions Sr^{2+}, Ba^{2+}, Cr^{3+}, and Fe^{3+} at a stoichiometry of 2:1 (PTU to metal ion) at 65 °C was done to generate four metal-based complexes of PTU. Then, the generated metal-based complexes of PTU were characterized by several physicochemical techniques, including CHN elemental analysis, ultraviolet/visible (UV-Visible) and Fourier-transform infrared (FT-IR) spectroscopies, X-ray diffraction (XRD), scanning and transmission electron (SEM), and thermal measurements.

EXPERIMENTAL

Chemicals

The investigated meal ions in chloride form were provided by Fluka Company (Seelze, Germany) as $SrCl_2{\cdot}6H_2O$ (266.62 g/mol), $BaCl_2{\cdot}2H_2O$ (244.26 g/mol), $CrCl_3{\cdot}6H_2O$ (266.45 g/mol), and $FeCl_3{\cdot}6H_2O$ (270.30 g/mol). These chlorides were of analytical grade chemicals and obtained with purities of 99.99%, ≥99%, ≥ 98.0%, and ≥ 98.0%, respectively. Merck KGaA (Darmstadt, Germany) provided 1-phenyl-2-thiourea (PTU; $C_6H_5NHCSNH_2$; 152.22 g/mol) in high purity (≥ 98.0%). Solvents used in the preparation were HPLC-grade methanol obtained from Sigma-Aldrich (St Louis, MO, USA), and deionized water from Water purification unit (Milli-Q system).

Synthesis

The PTU complexes were synthesized using the chemical reaction of PTU with the metal ions Sr^{2+}, Ba^{2+}, Cr^{3+}, and Fe^{3+} at stoichiometry of 2:1 (PTU to metal ion) at temperature of 65 °C. Each aqueous solution of $SrCl_2{\cdot}6H_2O$, $BaCl_2{\cdot}2H_2O$, $CrCl_3{\cdot}6H_2O$, and $FeCl_3{\cdot}6H_2O$ (1.0 mmol; 20 mL) were mixed well with a hot methanolic solution of PTU (2.0 mmol; 20 mL). The four mixtures (Sr^{2+}-PTU, Ba^{2+}-PTU, Cr^{3+}-PTU, and Fe^{3+}-PTU) were refluxed at 65 °C under stirring for 20 minutes. The resulting precipitates were filtrated off, washed three times with methanol, and dried in vacuum desiccators over anhydrous $CaCl_2$ for 48 h. The metal-based complex of PTU obtained with Sr^{2+} ions was termed Complex 1, the one obtained with Ba^{2+} ions was termed Complex 2, the one obtained with Cr^{3+} ions was termed Complex 3, and the last one was termed Complex 4.

Physicochemical characterizations

Several physicochemical techniques were used to characterize the synthesized metal-based complexes of PTU structurally, thermally, and morphologically. The structural characteristics of the complexes were assessed using Perkin-Elmer 2400 series II CHNS elemental analyzer for carbon, nitrogen, and hydrogen contents (%), Perkin-Elmer Lambda 25 UV/Vis spectrophotometer for electronic spectra scanned over the wavelength range from 200 to 1000 nm, Shimadzu Fourier-transform infrared spectrophotometer for FT-IR spectra scanned over the wavenumber from 400 to 4000 cm^{-1}. The phase purity and morphological properties were evaluated using X'Pert Philips X-ray diffractometer and Thermo Fisher Scientific high resolution Scanning Electron Microscope with environmental mode (Quattro ESEM). The thermal properties of the complexes were assessed using Shimadzu TG/DTG-50H thermal analyzer. The thermograms of the complexes were collected in the temperature range 25-600 °C.

RESULTS AND DISCUSSION

CHNS elemental analysis and UV-visible data

Carbon, nitrogen, hydrogen, and sulfur contents in complexes 1, 2, 3, and 4 were determined by CHNS elemental analyzer, where water and metal contents were obtained gravimetrically. Microanalytical data for Complex 1: calc. (found) for Sr, 16.38% (16.15); Water, 13.46% (13.70); N, 10.47% (10.60); S, 11.96% (12.12); C, 31.40% (31.22); and H, 4.49% (4.35). Microanalytical data for Complex 2: calc. (found) for Ba, 23.50% (23.33); Water, 12.32% (12.51); N, 9.59% (9.72); S, 10.95% (11.20); C, 28.76% (28.88); and H, 4.11% (4.35). Microanalytical data for Complex 3: calc. (found) for Cr, 9.11% (9.30); Water, 18.92% (18.70); N, 9.81% (9.99); S, 11.21% (11.10); C, 29.43% (29.30); and H, 4.90% (5.16). Microanalytical data for Complex 4: calc. (found) for Fe, 9.72% (9.94); Water, 18.79% (18.90); N, 9.75% (9.52); S, 11.14% (11.03); C, 29.24% (29.38); and H, 4.87% (5.06). The microanalytical data suggest that the synthesized complexes of Sr^{2+}, Ba^{2+}, Cr^{3+}, and Fe^{3+} can be formulated as $[Sr(PTU)_2(H_2O)_4]\cdot Cl_2$, $[Ba(PTU)_2(H_2O)_4]\cdot Cl_2$, $[Cr(PTU)_2(H_2O)_2Cl_2]\cdot Cl\cdot 4H_2O$, and $[Fe(PTU)_2(H_2O)_2Cl_2]\cdot Cl\cdot 4H_2O$, respectively. These formulas were corresponding to gross formulas of $C_{14}H_{24}N_4S_2O_4Cl_2Sr$ (534.96 g/mol), $C_{14}H_{24}N_4S_2O_4Cl_2Ba$ (584.23 g/mol), $C_{14}H_{28}N_4S_2O_6Cl_3Cr$ (570.79 g/mol), and $C_{14}H_{28}N_4S_2O_6Cl_3Fe$ (574.63 g/mol), respectively.

The synthesized PTU complexes were dissolved in dimethylsulfoxide (DMSO) solvent, and the resulting solutions were scanned by a UV/Vis spectrophotometer. The collected electronic spectra are shown in Figure 1. All complexes displayed multi- absorption bands with different intensity and width. The UV-Visible spectrum of Complex 1 contains three absorption bands. The first band is the strongest and broad band located at 230 nm, the second and the third absorption bands appeared at 250 and 260 nm and have the same intensity and width. Complex 2 gave four absorption bands. The first three bands located at 215, 225, and 245 nm. These bands have the same intensity and width. The fourth absorption band appeared at 260 nm. It is the most intense and widest band. Complex 3 exhibits five absorption bands. The first and the fifth absorption bands have the same intensity and width and located at 210 and 275 nm. The second and the fourth absorption bands have the same intensity and width. These two bands were located at 232 and 258 nm and were the most intensity and broad than the other bands. The third absorption band centered at 245 nm, and it's the less intensity and width than the other bands. All these absorptions can be attributed to the $\pi\rightarrow\pi^*$ transitions. Complex 4 displayed three absorption bands at 232, 250, and 270 nm. These three bands have different intensity and width. The most intense and widest band is that located at 250 nm.

FTIR spectroscopy

The FTIR frequencies (cm^{-1}) and mode of vibrations for the free PTU ligand and the synthesized complexes were presented in Table 1. The free PTU ligand shows the following characteristic absorption bands in its FTIR spectrum: (i) N–H vibrations: Absorption bands located at 3424, 3278 and 3182 cm^{-1} were due to the asymmetric and symmetric stretching vibrations of $-NH_2$ group. The bending modes of $-NH_2$ (rocking, twisting, wagging, and scissoring) had appeared at 694, 1166, 1318, and (1611 and 1588) cm^{-1} due to the $\delta_{rock}(NH_2)$, $\delta_{twist}(NH_2)$, $\delta_{wag}(NH_2)$, and $\delta_{sciss}(NH_2)$, respectively [23]. (ii) C–H vibrations: Bands observed at 3040 and 3003 cm^{-1} were attributed to the asymmetric and symmetric stretching vibrations of C–H of the phenyl ring. The bending deformations of C–H had appeared exactly at 1487, 983, 811, and 760 cm^{-1}. (iii) C=C vibrations: Absorption bands centered at 1533, and 1520 cm^{-1} were assigned to the ν(C=C) vibrations. (iv) C–N vibrations: Bands observed at 1464, 1297, 1276, and 1075 cm^{-1} resulted from the asymmetric and symmetric stretching vibrations of C–N groups [23]. (v) C=S vibrations:

Bands located at 1445, and 713 cm^{-1} were attributed to the $\nu_{as}(C=S)$ and $\nu_{s}(C=S)$, respectively, while band at 500 cm^{-1} was due to the $\delta(C=S)$ deformation.

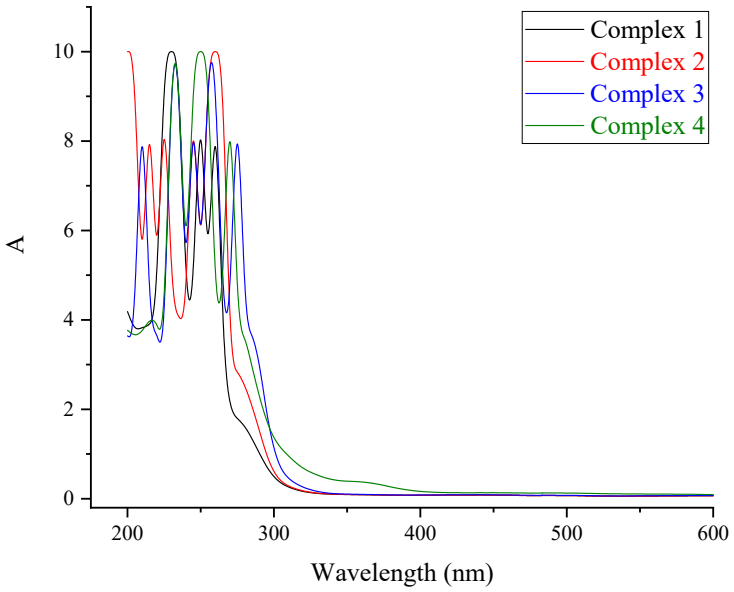

Figure 1. UV-Visible spectra of the manufactured complexes 1, 2, 3, and 4.

After complexation between PTU and the investigated metal ions, the frequencies resulted from the $-NH_2$ modes [$\nu_{as}(NH_2)$, $\nu_{s}(NH_2)$, $\delta_{rock}(NH_2)$, $\delta_{twist}(NH_2)$, $\delta_{wag}(NH_2)$, and $\delta_{sciss}(NH_2)$] were slightly shifted or remained in the same position as observed in the free PTU. The frequency of the $\nu_{as}(C=S)$ vibrations was significantly moved from 1445 cm^{-1} in the free PTU to 1397 cm^{-1} in Complex 1, to 1390 cm^{-1} in Complex 2, to 1385 cm^{-1} in Complex 3, and to 1387 cm^{-1} in Complex 4. The band of $\delta(C=S)$ vibrations occurs near 500 cm^{-1} in the free PTU was shifted to 553, 550, 552, and 549 cm^{-1} in complexes 1, 2, 3, and 4, respectively. Bands registered at 480, 492, 485, and 483 cm^{-1} in IR spectra of Complex 1, Complex 2, Complex 3, and Complex 4, respectively, could be assigned to the $\nu(C=S\ldots M)$ vibrations. All the four angular deformation motion of coordinated water molecules were found in the FTIR spectra of complexes. The vibration of $\delta_{twist}(H_2O)$ was appeared in the range of 583-580 cm^{-1}, that of the $\delta_{wag}(H_2O)$ vibration was found in the range of 675-670 cm^{-1}, that of the $\delta_{rock}(H_2O)$ vibration was noticed within the range of 850-847 cm^{-1}, and that of the $\delta_{b}(H_2O)$ vibration was detected within the range of 1638-1635 cm^{-1} [24]. Based on the analytical and spectral measurements, proposed structures of complexes 1, 2, 3, and 4 were shown in Figures 2 and 3.

Table 1. The FTIR frequencies (cm^{-1}) and mode of vibrations for the synthesized PTU meal complexes.

Wavelength (cm^{-1})					Mode of vibration
Free PTU ligand	Complex 1	Complex 2	Complex 3	Complex 4	
3424	3417	3419	3420	3418	$\nu_{as}(NH_2)$
3278	3265	3269	3270	3268	$\nu_{as}(NH_2)$
3182	3183	-	3170	3177	$\nu_s(NH_2)$
3040, 3003	2980	3034, 3010	3005	3033	$\nu_{as}(C–H) + \nu_s(C–H)$
-	1637	1635	1638	1635	$\delta_b(H_2O)$
1617	1615	1622	-	1618	νPh; phenyl ring
1611	1610	1608	1609	1610	$\delta_{sciss}(NH_2)$
1594	1594	1593	1590	1596	νPh; phenyl ring
1588	1585	-	-	1584	$\delta_{sciss}(NH_2)$
1533, 1520	1518	1523	-	1519	ν(C=C)
1506	1500	1502	1505	-	νPh; phenyl ring
1487	-	1495	1490	1493	$\delta_{def}(C–H)$
1464	1462	1465	1458	1460	$\nu_{as}(C–N)$
1445	1397	1390	1385	1387	$\nu_{as}(C=S)$
1318	1311	1312	1315	-	$\delta_{wag}(NH_2)$
1297	1293	1293	1296	1295	$\nu_{as}(C–N)$
1276	1274	1273	-	1275	$\nu_{as}(C–N)$
1166	1168	1172	1171	1170	$\delta_{twist}(NH_2)$
1115	-	-	1123	1118	Ring breathing mode
1075	1055	1058	1056	1055	$\nu_s(C–N)$
1062	1033	1025	1024	1030	Ring breathing mode
983	1014, 918	1002, 931	1001	1010, 915	$\delta_{def}(C–H)$
-	847	848	850	850	$\delta_{rock}(H_2O)$
713	747	748	746	748	$\nu_s(C=S)$
694	690	694	691	695	$\delta_{rock}(NH_2)$
-	672	675	672	670	$\delta_{wag}(H_2O)$
639	633	636	634	635	δ(N–C–S)
614, 605	602	603	603	605	Out-of-plane ring deformation γPh
-	580	583	580	582	$\delta_{twist}(H_2O)$
500	553	550	552	549	δ(C=S)
-	480	492	485	483	(M–O)
460	465	464	463	462	δ(N–C–N)

XRD diffractometry

Complexes of PTU with the investigated metal ions were scanned by an XRD instrument, and the spectral data obtained from the XRD patterns of the complexes are tabulated in Table 2. Complex 1 displayed two characteristic XRD reflections with a very strong and medium intensity that was observed at Bragg's angle 2θ value of 19.8585°, and 23.9622°, respectively. The XRD diffractogram of Complex 1 also showed a group of low-intensity lines. The XRD profile of Complex 2 displayed five diffraction lines in the range from 14° to 45°; these reflections had appeared at 2θ values of 19.1221° (very strong), 16.1279° (medium strong), 23.6034° (medium strong), 30.5950° (medium), and 35.2325° (medium). The XRD patterns of Complex 3 exhibited a single very strong, and narrow sharp diffraction pattern at a 2θ 19.6637°. Complex 3 also displayed a low intensity XRD reflection at 23.9220°. The obtained reflections suggests that

Complex 3 had a well-organized and well-defined structure. The XRD spectrum of Complex 4 contains three characteristic reflections located exactly at Bragg's angle 2θ values of 19.3560° (very strong), 23.4371° (strong), and 25.6499° (medium). The full width at half-maximum (FWHM) of the strongest diffraction line for the complexes 1, 2, 3, and 4 were 0.48170°, 0.56010°, 0.49920°, and 0.62970°, respectively. Values of the inter-planar spacing between the atoms (*d*-spacing) of the highest-intensity line were 4.46727 Å, 4.63761 Å, 4.51108 Å, and 4.58209 Å for complexes 1, 2, 3, and 4, respectively.

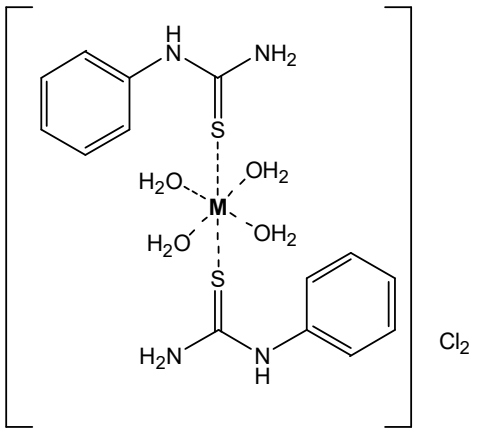

Figure 2. Proposed chemical structures of complexes 1 and 2 (M: Sr^{2+}, Ba^{2+}).

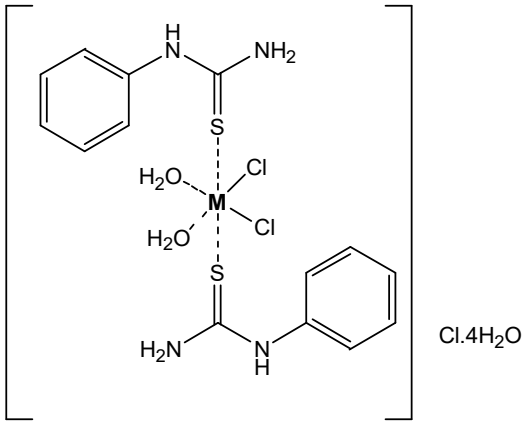

Figure 3. Proposed chemical structures of complexes 3 and 4 (M: Cr^{3+}, Fe^{3+}).

SEM images

SEM images capture at different levels of magnification for complexes 1, 2, 3, and 4 are presented in Figures 4, 5, 6, and 7, respectively. These images were used to collect specific outer surface-related data for the synthesized complexes including microstructure, surface topology, shape and size of particles, and the possibility of existing porous structure on the surface. The SEM images

of Complex 1 indicated that it consisted of small particles with varying shapes and sizes. Some of the complex's particles were fused together, forming solid, big pieces. Particles of Complex 2 had rod-like morphology. These rods were mixed between short and long rods. Some of these rods were broken into small pieces. A kind of deformation had occurred to some of the Complex 2's rods. The magnified images (x10,000 and x20,000) indicated that Complex 3 had sponge-like texture with several clear holes. The SEM images of Complex 4 indicated that it consisted of big pieces with different shape and size. Some of these pieces exhibited sharp edges.

Table 2. The XRD spectral data of the strongest three peaks for complexes 1, 2, 3, and 4.

Complex	XRD data					
	Peak no.	2θ (deg)	*d*-spacing value; (Å)	Intensity (I/I1)	FWHM (deg)	Intensity (Counts)
Complex 1	5	19.8585	4.46727	100	0.48170	875
	8	23.9622	3.71070	53	0.57840	463
	14	34.1313	2.62482	31	0.87870	271
Complex 2	5	19.1221	4.63761	100	0.56010	2720
	9	23.6034	3.76629	55	0.55560	1508
	3	16.1279	5.49123	46	0.62230	1238
Complex 3	2	19.6637	4.51108	100	0.49920	3128
	4	23.9220	3.71684	27	0.61300	855
	5	25.9889	3.42574	7	1.07210	219
Complex 4	5	19.3560	4.58209	100	0.62970	969
	8	23.4371	3.79263	83	0.61710	808
	10	25.6499	3.47024	51	0.67960	492

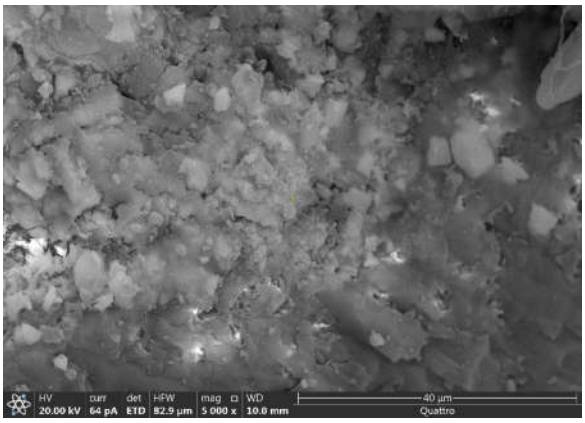

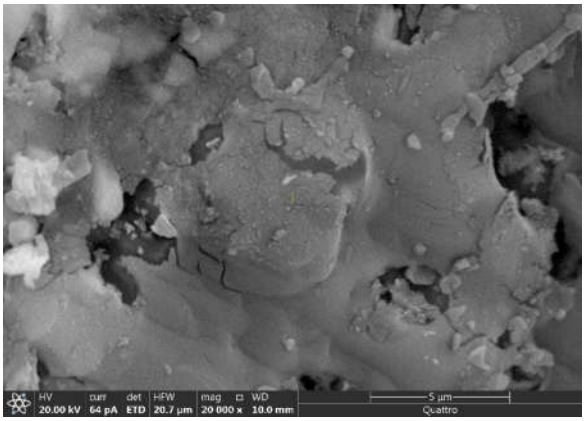

Figure 4. SEM images of Complex 1.

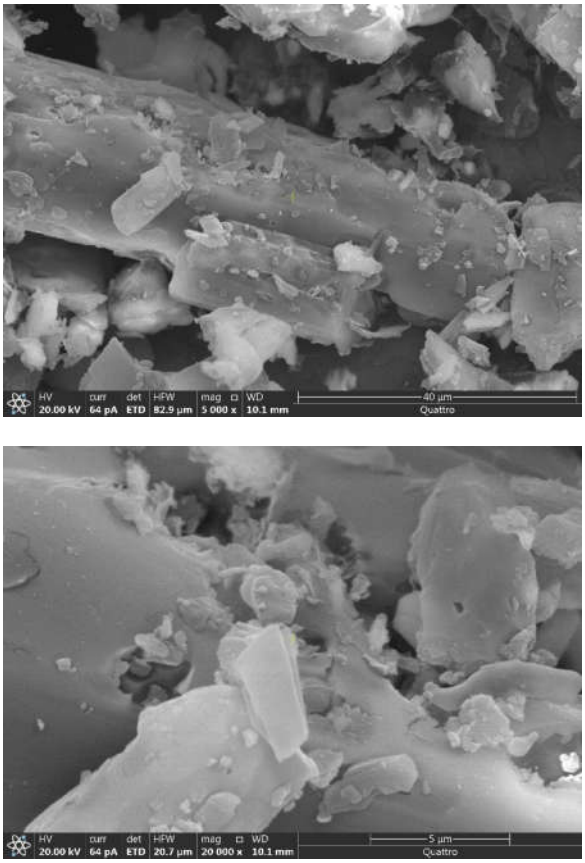

Figure 5. SEM images of Complex 2.

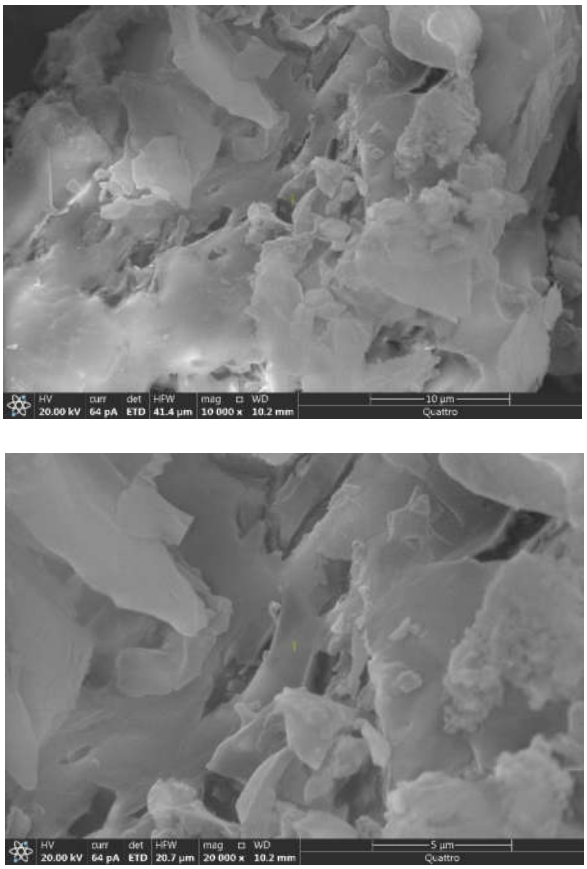

Figure 6. SEM images of Complex 3.

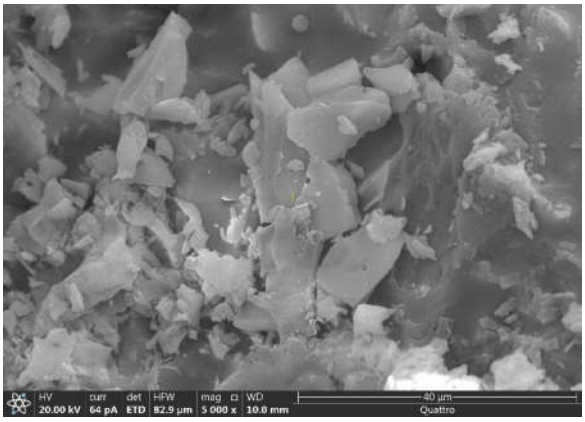

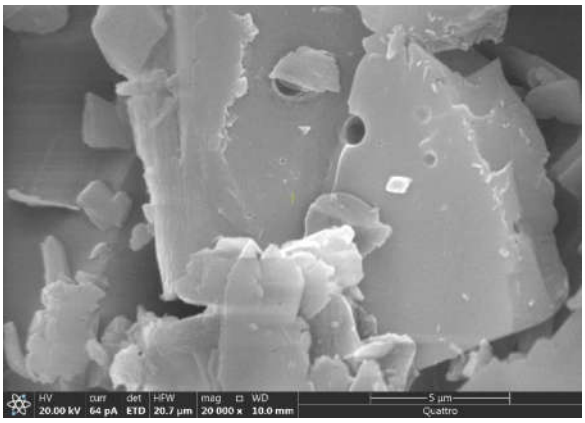

Figure 7. SEM images of Complex 4.

Thermogravimetry

The thermal properties of the synthesized complexes were assessed using a Shimadzu TG/DTG-50H thermal analyzer. The thermograms of complexes 1, 2, 3, and 4 were collected in the temperature range 25-600 °C. From the collected thermograms, Complex 1, Complex 2, Complex 3, and Complex 4 were found to be thermally stable up to 135, 75, 75, and 120 °C, respectively. Complexes 2 and 4 were decomposed in two-steps decomposition patterns in temperature range of 75-200 °C and 200-400 °C for Complex 2, and in temperature range of 120-360 °C and 360-600 °C for Complex 4. Complex 1 was thermally decomposed in a one-stage degradation step (135-400 °C), while Complex 3 was thermally decomposed in three-stage degradation steps (75-200, 200-400, and 400-600 °C). The degradation steps of complexes 1 and 2 were completed by leaving $SrCO_3$ and $BaCO_3$, respectively, whereas the degradations of complexes 3 and 4 were completed by leaving Cr_2O_3 and Fe_2O_3, respectively. The weight losses corresponded with the degradation steps of Complex 2 were as follows: (found =24.50, cal. =24.45%) for step one and (found =49.37, cal. =49.98%) for step two. The weight losses corresponded with the degradation steps of Complex 3 were as follows: (found =18.64, cal. =18.92%) for step one, (found =18.89, cal. =18.80%) for step two, and (found =52.75, cal. =53.08%) for step three. The weight losses corresponded with the degradation steps of Complex 4 were as follows: (found =37.06, cal. =37.47%) for step one and (found =52.38, cal. =52.72%) for step two. Complex 1 was decomposed in one step start at 135 °C and complete at 400 °C, associated with a weight loss of (found =81.07, cal.=81.29).

CONCLUSION

Four complexes of 1-phenyl-2-thiourea as a ligand (termed PTU) were prepared from the reaction of the metal ions Sr^{2+}, Ba^{2+}, Cr^{3+}, and Fe^{3+} with the ligand at a stoichiometry of 2:1 (PTU to metal ion) and a temperature of 65°C. This reaction generated thermally stable metal-based complexes, which referred to as Complex 1 (Sr^{2+}), Complex 2 (Ba^{2+}), Complex 3 (Cr^{3+}), and Complex 4 (Fe^{3+}). After the preparation of the complexes, they were characterized by several analytical methods, including elemental analyses, X-ray diffraction (XRD), thermogravimetry (TG), spectroscopies (UV-visible and FT-IR), and scanning electron microscope with environmental mode (ESEM). Analytical results suggested that the manufactured complexes can be formulated as $[Sr(PTU)_2(H_2O)_4]\cdot Cl_2$ (Complex 1), $[Ba(PTU)_2(H_2O)_4]\cdot Cl_2$ (Complex 2), $[Cr(PTU)_2(H_2O)_2Cl_2]\cdot Cl\cdot 4H_2O$ (Complex 3), $[Fe(PTU)_2(H_2O)_2Cl_2]\cdot Cl\cdot 4H_2O$ (Complex 4). The

XRD and ESEM results demonstrated that the complexes exhibited high purity and possessed a uniform and well-structured morphology.

ACKNOWLEDGMENT

The authors extend their appreciation to Taif University, Saudi Arabia, for supporting this work through project number (TU-DSPP-2024-78).

FUNDING

This research was funded by Taif University, Saudi Arabia, Project No. (TU-DSPP-2024-78).

REFERENCES

1. El-Habeeb, A.A.; Refat, M.S. Synthesis, spectroscopic characterizations and biological studies on gold(III), ruthenium(III) and iridium(III) complexes of trimethoprim antibiotic drug. *Bull. Chem. Soc. Ethiop.* **2024**, 38, 701-714.
2. Alsuhaibani, A.M.; Adam, A.M.A.; Refat, M.S.; Kobeasy, M.I.; Bakare, S.B.; Bushara, E.S. Spectroscopic, thermal, and anticancer investigations of new cobalt(II) and nickel(II) triazine complexes. *Bull. Chem. Soc. Ethiop.* **2023**, 37, 1151-1162.
3. Younes, A.A.O.; Refat, M.S.; Saad, H.A.; Adam, A.M.A.; Alzoghibi, O.M.; Alsulaim, G.M.; Alsuhaibani, A.M. Complexation of some alkaline earth metals with bidentate uracil ligand: Synthesis, spectroscopic and antimicrobial analysis. *Bull. Chem. Soc. Ethiop.* **2023**, 37, 945-957.
4. Alkathiri, A.A.; Atta, A.A.; Refat, M.S.; Altalhi, T.A.; Shakya, S.; Alsawat, M.; Adam, A.M.A.; Mersal, G.A.M.; Hassanien, A.M. Preparation, spectroscopic, cyclic voltammetry and DFT/TD-DFT studies on fluorescein charge transfer complex for photonic applications. *Bull. Chem. Soc. Ethiop.* **2023**, 37, 515-532.
5. Adam, A.M.A.; Refat, M.S.; Gaber, A.; Grabchev, I. Complexation of alkaline earth metals Mg^{2+}, Ca^{2+}, Sr^{2+} and Ba^{2+} with adrenaline hormone: Synthesis, spectroscopic and antimicrobial analysis. *Bull. Chem. Soc. Ethiop.* **2023**, 37, 357-372.
6. Al-Hazmi, G.H.; Adam, A.M.A.; El-Desouky, M.G.; El-Bindary, A.A.; Alsuhaibani, A.M.; Refat, M.S. Efficient adsorption of Rhodamine B using a composite of Fe_3O_4@zif-8: Synthesis, characterization, modeling analysis, statistical physics and mechanism of interaction. *Bull. Chem. Soc. Ethiop.* **2023**, 37, 211-229.
7. Alsuhaibani, A.M.; Adam, A.M.A.; Refat, M.S. Four new tin(II), uranyl(II), vanadyl(II), and zirconyl(II) alloxan biomolecule complexes: Synthesis, spectroscopic and thermal characterizations. *Bull. Chem. Soc. Ethiop.* **2022**, 36, 373-385.
8. Al-Hazmi, G.H.; Alibrahim, K.A.; Refat, M.S.; Ibrahim, O.B.; Adam, A.M.A.; Shakya, S. A new simple route for synthesis of cadmium(II), zinc(II), cobalt(II), and manganese(II) carbonates using urea as a cheap precursor and theoretical investigation. *Bull. Chem. Soc. Ethiop.* **2022**, 36, 363-372.
9. Alsuhaibani, A.M.; Refat, M.S.; Adam, A.M.A.; Kobeasy, M.I.; Kumar, D.N.; Shakya, S. Synthesis, spectroscopic characterizations and DFT studies on the metal complexes of azathioprine immunosuppressive drug. *Bull. Chem. Soc. Ethiop.* **2022**, 36, 73-84.
10. El-Sayed, M.Y.; Refat, M.S.; Altalhi, T.; Eldaroti, H.H.; Alam, K. Preparation, spectroscopic, thermal and molecular docking studies of covid-19 protease on the manganese(II), iron(III), chromium(III) and cobalt(II) creatinine complexes. *Bull. Chem. Soc. Ethiop.* **2021**, 35, 399-412.

11. Alosaimi, A.M.; Saad, H.A.; Al-Hazmi, G.H.; Refat, M.S. In situ acetonitrile/water mixed solvents: An ecofriendly synthesis and structure Explanations of Cu(II), Co(II), and Ni(II) complexes of thioxoimidazolidine. *Bull. Chem. Soc. Ethiop.* **2021**, 35, 351-364.
12. Refat, M.S.; Altalhi, T.A.; Al-Hazmi, G.H.; Al-Humaidi, J.Y. Synthesis, characterization, thermal analysis and biological study of new thiophene derivative containing o-aminobenzoic acid ligand and its Mn(II), Cu(II) and Co(II) metal complexes. *Bull. Chem. Soc. Ethiop.* **2021**, 35, 129-140.
13. Cao, Q.; Li, Y.; Freisinger, E.; Qin, P.Z.; Sigel, R.K.O.; Mao, Z-W. G-quadruplex DNA targeted metal complexes acting as potential anticancer drugs. *Inorg. Chem. Front.* **2017**, 4, 10-32.
14. Trudu, F.; Amato, F.; Vaňhara, P.; Pivetta, T.; Peña-Méndez, E.M.; Havel, J. Coordination compounds in cancer: Past, present and perspectives. *J. Appl. Biomed.* **2015**, 13, 79-103.
15. Mjos, K.D.; Orvig, C. Metallodrugs in medicinal inorganic chemistry. *Chem. Rev.* **2014**, 114, 4540-4563.
16. Alessio, E. *Bioinorganic Medicinal Chemistry*, Wiley-VCH Verlag GmbH: New York; **2011**.
17. Tella, A.C.; Obaleye, J.A.; Olawale, M.D.; Ngororabanga, J.M.V.; Ogunlaja, A.S.; Bourned, S.A. Synthesis, crystal structure, and density functional theory study of a zinc(II) complex containing terpyridine and pyridine-2,6-dicarboxylic acid ligands: Analysis of the interactions with amoxicillin. *C.R. Chimie* **2019**, 22, 3-12.
18. Eichhorn, G.L.; Marzilli, L.G. *Advances in Inorganic Biochemistry Models in Inorganic Chemistry*, PTR Prentice-Hall, Inc.: New Jersey; **1994**.
19. Hughes, M.N. *The Inorganic Chemistry of Biological Processes*, 2nd ed., Wiley: Chichester England; **1984**.
20. Shakeel, A.; Altaf, A.A.; Qureshi, A.M.; Badshah, A. Thiourea derivatives in drug design and medicinal chemistry: A short review. *J. Drug Design Med. Chem.* **2016**, 2, 10-20.
21. Rigaudy, J.; Klesney, S.; Rigaudy, *J. Nomenclature of Organic Chemistry*: Sections A, B, C, D, E, F and H: Pergamon Press: Oxford; **1979**.
22. Wahid, A.; Basran, S.M.A.; Farooq, M.; Wahid, A.; Basra, S.M.A.; Farooq, M. Thiourea: a molecule with immense biological significance for plants. *Int. J. Agric. Biol.* **2017**, 19, 911-920.
23. Panicker, C.Y.; Varghese, H.T.; George, A.; Thomas, P.K.V. FT-IR, FT-Raman and ab-initio studies of 1,3-diphenyl thiourea. *Eur. J. Chem.* **2010**, 1, 173-178.
24. Deacon, G.B.; Phillips, R.J. Relationships between the carbon-oxygen stretching frequencies of carboxylato complexes and the type of carboxylate coordination. *Coord. Chem. Rev.* **1980**, 33, 227-250.